Electron-Transfer Reorganization Energies of Isolated Organic Molecules†

Xenia Amashukeli,‡ Jay R. Winkler,*,‡ Harry B. Gray,*,‡ Nadine E. Gruhn,§ and Dennis L. Lichtenberger*,§

Division of Chemistry and Chemical Engineering and the Beckman Institute, California Institute of Technology, Pasadena, California 91125, and Department of Chemistry, University of Arizona, Tucson, Arizona 85721

Received: November 13, 2001; In Final Form: February 20, 2002

He I photoelectron spectra of phenanthrene (**1**), 1,10-phenanthroline (**2**), phenazine (**3**), dibenzo[*a*,*c*]anthracene (**4**), dibenzo[*a*,*c*]phenazine (**5**), and dipyrido[3,2-*a*;2′3′-*c*]phenazine (**6**) have been obtained. Assignment of the π ionization states was aided by electronic structure calculations: the first ionization state of **1**, $^2B_1(\pi_1)$, is observed at 7.888 ± 0.002 eV, $^2B_2(\pi_1)$ of **2** is at 8.342 ± 0.002 eV, and $^2B_{1g}(\pi_1)$ of **3** is at 8.314 ± 0.002 eV. Spectra of **4**−**6** are reported for the first time: $^2A_2(\pi_1)$ of **4** is at 7.376 ± 0.002 eV, and both **5** (7.983 ± 0.002 eV) and **6** (8.289 ± 0.002 eV) exhibit quasi-degenerate first and second ionization states. Quantum-mechanical reorganization energies, λ^{QM}, were extracted from analyses of vibrational structure: values are 149 ± 5 (**1**), 167 ± 5 (**2**), 68 ± 2 (**3**), and 92 ± 4 (**4**) meV. Low-frequency modes were treated semiclassically: values of λ^{SC} are estimated to be 21 ± 1 (**1**), 13 ± 1 (**2**), 22 ± 1 (**3**), 66 ± 1 (**4**), 27 ± 9 (**5**), and 16 ± 1 (**6**) meV. Reorganization energies ($\lambda = \lambda^{QM} + \lambda^{SC}$) of isolated molecules are 170 ± 5 (**1**), 180 ± 5 (**2**), 90 ± 2 (**3**), and 158 ± 4 (**4**) meV. Density functional calculations (B3LYP/6-311G++(d,p)) give λ values that are on average 63 meV lower than experimentally derived energies.

Introduction

Electron-transfer reactions are key steps in a vast array of chemical and biological processes.[1] According to semiclassical theory, the rates of these reactions in solution are governed by three fundamental parameters: the reorganization energy, λ (where $\lambda = \lambda_i + \lambda_o$, the inner- and outer-sphere contributions); the electronic coupling matrix element, H_{AB}, and the standard free energy change, $\Delta G°$.[2] Both theoretical and experimental investigations suggest that the solvent contribution (λ_o) to the reorganization energy is much larger in most cases than the inner-sphere contribution (λ_i). It also has been shown that the ratio λ_o/λ_i decreases with decreasing solvent polarity.[3] The limiting case is a reaction in the absence of bulk solvent, as occurs in the gas phase.[4]

In this paper, we report reorganization energies that were extracted from analyses of the photoelectron spectra of six isolated organic molecules: phenanthrene (**1**), 1,10-phenanthroline (**2**), phenazine (**3**), dibenzo[*a*,*c*]anthracene (**4**), dibenzo[*a*,*c*]phenazine (**5**), and dipyrido[3,2-*a*;2′3′-*c*]phenazine (**6**) (Scheme 1). These particular molecules were selected because they are often employed as redox active components in donor-bridge-acceptor systems.[5]

Experimental Section

Materials. 1−4 were obtained from Aldrich. **5** was prepared by refluxing 9,10-phenanthrenequinone (3 mmol) and 1,2-diaminobenzene (3 mmol) in dry methanol. A sample of **6** was kindly provided by Sarah Delaney (Caltech).

Photoelectron Spectroscopy. He I photoelectron spectra were recorded using an instrument with a 36-cm diameter, 8-cm gap hemispherical analyzer (McPherson). The ionization source, detection, and control electronics have been described in detail elsewhere.[6,7] The ionization energy scale was calibrated using the $^2E_{1/2}$ ionization of methyl iodide (9.538 eV), with the Ar $^2P_{3/2}$ ionization (15.759 eV) used as an internal energy scale lock during data collection. During data collection, the instrument resolution, measured as full-width-at-half-maximum of the Ar $^2P_{3/2}$ ionization, was 0.019−0.025 eV for **1**−**4** and **6** and 0.033 eV for **5**. Since the He I discharge source is not monochromatic,[8] the spectra collected with He Iα ($1s^2 \leftarrow 1s2p$, 21.218 eV) source were corrected for He Iβ line ($1s^2 \leftarrow 1s3p$, 23.085 eV, and 3% of the intensity of the He Iα line). Data collection temperatures ($\sim 10^{-4}$ Torr, monitored using a "K" type thermocouple passed through a vacuum feed and attached directly to the ionization cell): phenanthrene, 47−58 °C; 1,-10-phenanthroline, 102−108 °C; phenazine, 63−83 °C; dibenzo-[*a*,*c*]anthracene, 141−152 °C; dibenzo[*a*,*c*]phenazine, 156−172 °C; dipyrido[3,2-*a*;2′3′-*c*]phenazine, 183−201 °C.

SCHEME 1

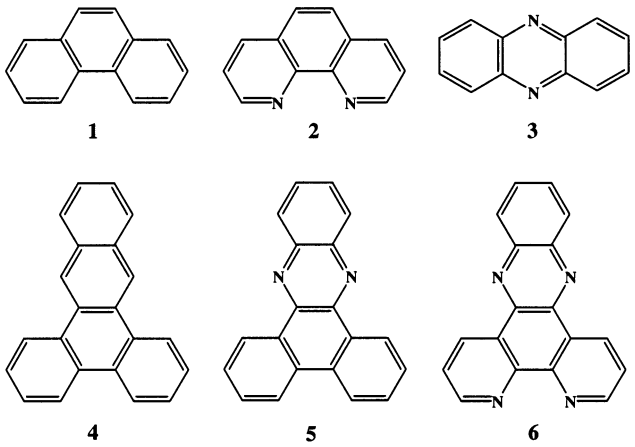

1 **2** **3** **4** **5** **6**

† Part of the special issue "G. Wilse Robinson Festschrift".
‡ California Institute of Technology.
§ University of Arizona.

10.1021/jp014148w CCC: $22.00
Published on Web 04/10/2002

TABLE 1: Ionization Energies (eV)

bands	IE(obsd)[a]	IE(calcd, raw)[b]	IE(calcd, compressed)[c]	IE(obsd) (ref 18)
		1		
B_1 (π_1)	7.888	7.751	7.888	7.87
A_2 (π_2)	8.289	8.059	8.123	(8.30)[d]
A_2 (π_3)	9.277	9.556	9.276	9.28
B_1 (π_4)	9.872	10.429	9.940	9.90
		2		
B_2 (π_1)	8.342	8.227	8.342	8.35
A_2 (π_2)	8.523	8.643	8.662	(8.82)[d]
σ_N	(9.433)[d]			9.39
		3		
B_{1g} (π_1)	8.314	8.150	8.314	8.33
B_{2g} (π_2)	8.928	8.703	8.739	(9.06)[d]
A_u (π_3)	9.519	9.765	9.556	9.56
σ_N	(9.158)[d]			9.2
		4		
A_2 (π_1)	7.376	7.250	7.376	
B_1 (π_2)	7.880	7.808	7.805	
A_2 (π_3)	8.254	8.325	8.203	
A_2 (π_4)	9.114	9.539	9.137	
B_1 (π_5)	9.367	9.862	9.385	
B_1 (π_6)	9.899	10.502	9.877	
		5		
A_2 (π_1)	7.983	8.007	7.983	
B_1 (π_2)		8.052	8.018	
A_2 (π_3)	8.589	8.651	8.478	
A_2 (π_4)	9.318	9.719	9.300	
B_1 (π_5)	9.676	10.143	9.626	
B_1 (π_6)	10.016	10.691	10.048	
		6		
A_2 (π_1)	8.289	8.332	8.289	
B_1 (π_2)		8.335	8.291	
A_2 (π_3)	9.106	9.289	9.025	
A_2 (π_4)	9.997	10.567	10.008	
B_1 (π_5)	10.265	10.888	10.255	

[a] Vertical ionizations; this work. The error in the ionization energy measurements was determined by fitting 12 individual scans of the photoelectron spectra of **1** with a series of Gaussian functions. Since all the measurements were carried out under similar conditions and the instrument resolution was nearly the same in all cases, the same error, ±0.002, was applied to the rest of the ionization energy values. [b] Calculated using RHF/6-311G++(2d,2p). [c] Calculated values are shifted to match the first ionization energy and compressed by a factor of 1.3 (ref 16). [d] Tentative experimental assignment.

Computational Details. Electronic structure calculations were carried out using Jaguar 4.1[9] and GAUSSIAN 98[10] programs. The geometries of all the molecules were optimized using the Becke three-parameter Lee−Yang−Parr functional (B3LYP) and 6-31G(d,p) basis sets. B3LYP consists of the hybrid exchange functional proposed by Becke[11] and the Lee−Yang−Parr[12] correlation functional. Reorganization energies were calculated using B3LYP/6-311G++(2d,2p) level of theory. Ionization energies were estimated from restricted Hartree−Fock (RHF) calculations with a 6-311G++(2d,2p) basis set (Table 1). Vibrational frequencies were calculated using B3LYP/6-31G(d,p) and scaled by 0.987 (for low-frequency modes) and 0.973 (for high-frequency modes) (Table 2).[13]

Results

Photoelectron spectra. He I spectra of **1**−**6** are shown in Figures 1 and 2. The data were fit with a series of Gaussian functions (eq 1, in which A is

$$T = A \exp(-\alpha)\left[\frac{(h\nu - p)}{H}\right]^2 \qquad (1)$$

TABLE 2: Selected Vibrational Frequencies (cm^{-1})

molecule	mode	ν(calcd) neutral	ν(calcd) cation	ν(obsd) neutral
1	$23a_1$	242	244	247[a]
	$22a_1$	405	401	408[a]/398[b]
	$21a_1$	549	547	548[a]
	$11a_1$	1356	1365	1352[a]/1340[b]
	$10a_1$	1426	1417	1431[a,b]
	$9a_1$	1441	1430	1443[a]/1446[b]
2	$21a_1$	237	233	249[c]
	$20a_1$	408	399	408[c]
	$19a_1$	554	547	550[c]
	$10a_1$	1349	1328	1343[c]
	$9a_1$	1387	1389	1404[c]
	$8a_1$	1450	1416	1444[c]
3	$6a_g$	1282	1268	1280[d]
	$5a_g$	1406	1395	1403[d]
	$4a_g$	1481	1486	1479[d]
4	$32a_1$	579	573	
	$31a_1$	632	624	
	$30a_1$	701	704	
	$17a_1$	1337	1356	
	$16a_1$	1372	1384	1360[e]
	$15a_1$	1405	1404	

[a] Polarized IR/Raman spectra of single-crystal phenanthrene (ref 19). [b] Gas-phase IR spectra of phenanthrene (ref 20). [c] Polarized IR/Raman spectra of single-crystal 1,10-phenanthroline (ref 21). [d] Polarized Raman spectra of single-crystal phenazine (ref 22). [e] IR spectra of thin solid films of dibenzo[*a*,*c*]anthracene (ref 23).

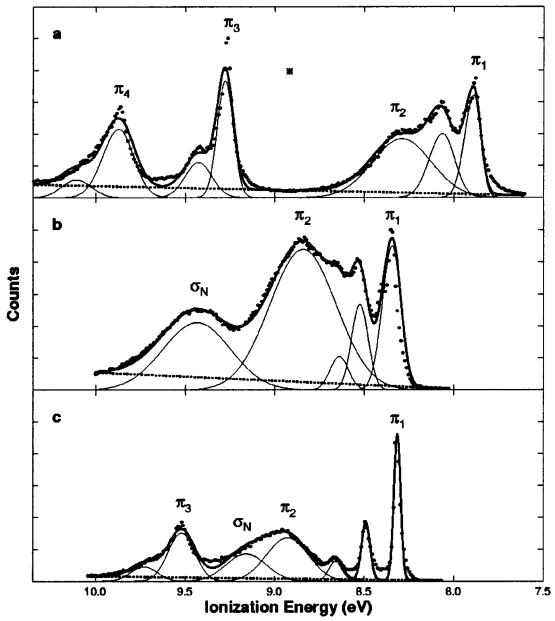

Figure 1. He I photoelectron spectra: (a) phenanthrene (**1**); (b) 1,-10-phenanthroline (**2**); (c) phenazine (**3**). Experimental data (···) are fit with Gaussian functions (−) on a baseline (···) giving total fit (−).

the peak height, p is the peak position, H is the average full-width at half-maximum, and α is $4\ln(2)$).[14] Sums of the Gaussian functions gave fits to the experimental data. Ionization energies of **1**−**6** are set out in Table 1. The bands were assigned to the ionization of π- or σ_N-electrons, where σ_N is the nitrogen lone pair state. Koopmans' theorem[15] aided the assignment of π-states. To compensate for the relaxation and electronic correlation effects that are neglected by Koopmans' theorem, the calculated energies were shifted to match the first experimental ionization energies and then compressed by the factor of 1.3.[16] σ_N-states were assigned on the basis of comparisons between diaza molecules and their carbon analogues. The σ_N-state in the phenazine spectrum was identified by comparison to the previously reported anthracene photoelectron spectrum.[17]

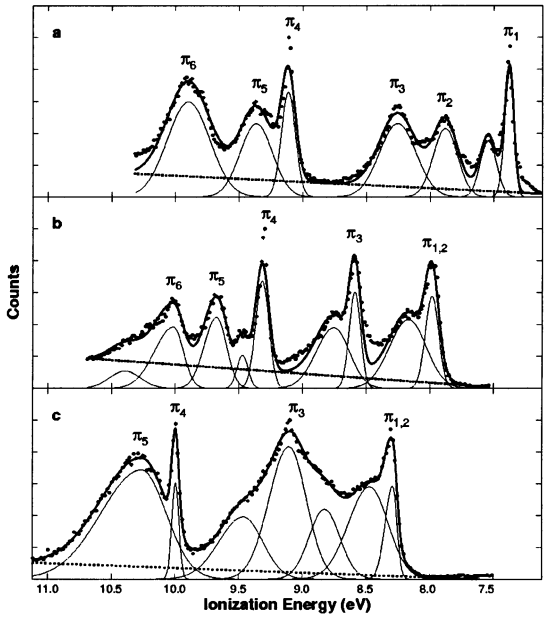

Figure 2. He I photoelectron spectra: (a) dibenzo[*a*,*c*]anthracene (**4**); (b) dibenzo[*a*,*c*]phenazine (**5**); (c) dipyrido[3,2-*a*; 2′3′−*c*]phenazine (**6**). Experimental data (···) are fit with Gaussian functions (−) on a baseline (···) giving total fit (—).

Since σ_N bands are broad, featureless, and low intensity, their assignment is tentative. The σ_N-states in **5** and **6** were not assigned due to spectral congestion. The first two ionizations of **5** are nearly degenerate; the bands are poorly resolved (the first band is at 7.983 ± 0.002 eV). Calculations suggest that the first and second ionizations of **6** are separated by 3 meV. These two bands, which were not experimentally resolved, are assigned an average value of 8.238 ± 0.002 eV.

Quantum-Mechanical Analysis (λ^{QM}). Quantum-mechanical analysis of fine structure in the spectra yielded distortion parameters (*S*), which are related to λ^{QM} according to eq 2 (*h* is

$$\lambda^{QM} = \sum_k S_k h\nu_k \qquad (2)$$

Planck's constant and ν_k is the vibrational frequency of mode *k*).[18] The first ionization bands in the spectra of **1**−**6** exhibit vibrational progressions (Figures 3−8). The bands in each spectrum were fit with a series of Gaussian functions; widths (*H*) of the vibrational components in each progression were kept fixed for molecules **1**−**4**. In all cases, hot bands were included as part of the fitting procedure.

The first ionization band of **1** exhibits a high-frequency progression (1455 ± 34 cm^{-1}) corresponding to the $10a_1$ mode, and a low-frequency progression (379 ± 34 cm^{-1}) arising from the $22a_1$ mode (Table 3). The first ionization band of **2** exhibits two vibrational progressions similar to those observed for **1**: a high-frequency progression with a spacing of 1461 ± 34 cm^{-1} and a low-frequency progression spaced by 420 ± 34 cm^{-1}. The first ionization band of **3** exhibits a well-resolved vibrational progression spaced by 1415 ± 34 cm^{-1} corresponding to the $5a_g$ mode (Table 3). The first ionization band of **4** is similar to those observed in the **1** and **2** spectra: a high-frequency progression (1357 ± 34 cm^{-1}) corresponding to the $16a_1$ mode and a low-frequency progression (632 ± 34 cm^{-1}) attributable to the $31a_1$ mode (Table 3).

We assume that the intensities of the individual Gaussian bands in each vibrational progression (Figures 3−6) follow a

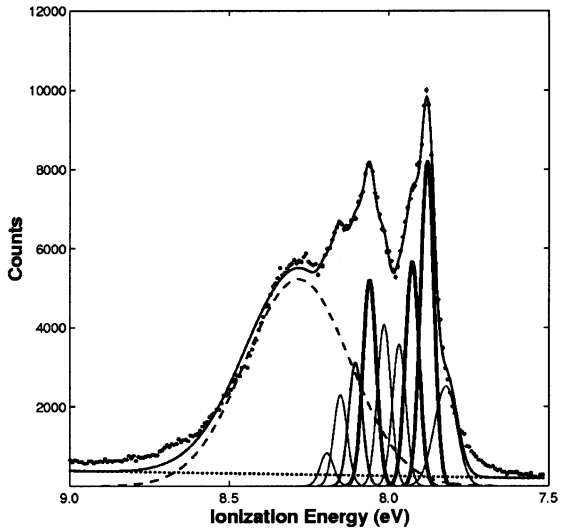

Figure 3. Low binding energy region in He I photoelectron spectrum of **1**. Experimental data (···) are fit with Gaussian functions corresponding to vibrational progressions (—) used in λ calculation, and π_2 ionization (- − -) on a baseline (···). Other Gaussian functions (−) describe spectral features of π_1.

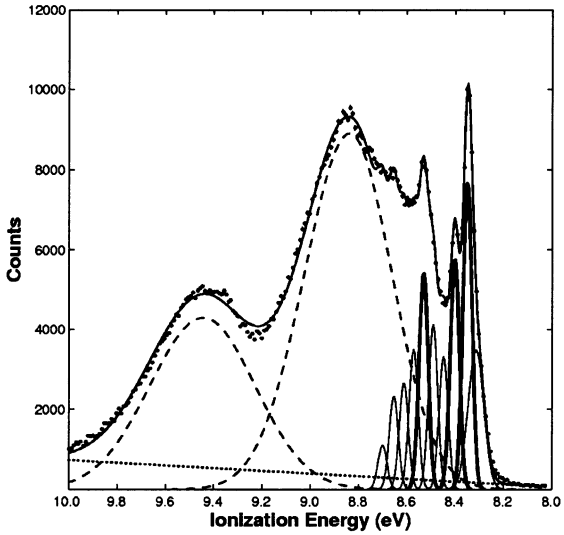

Figure 4. Low binding energy region in He I photoelectron spectrum of **2**. Experimental data (···) are fit with Gaussian functions corresponding to vibrational progressions (—) used in λ calculation, and π_2 and π_3 ionizations (- − -) on a baseline (···). Other Gaussian functions (−) describe spectral features of π_1.

Poisson distribution (eq 3, where I_n is the intensity of the *n*th

$$I_n = \frac{S^n}{n!}e^{-S} \qquad (3)$$

vibrational band).[24] Since only the first two vibrational bands are well-resolved, the values of *S* were extracted from the ratio of I_1 to I_0. The results are summarized in Table 3. According to the RHF/6-311G++(2d,2p) calculation (Table 1), the first and second ionization energies of **5** are nearly the same; although vibrational structure is present in the spectrum, it is difficult to determine the mode to which it corresponds. Thus, values of *S* were not obtained for this molecule. Similar problems complicated the analysis of the photoelectron spectrum of **6**.

Semiclassical Analysis (λ^{SC}). Distortions along low-frequency modes and small frequency changes between the neutral

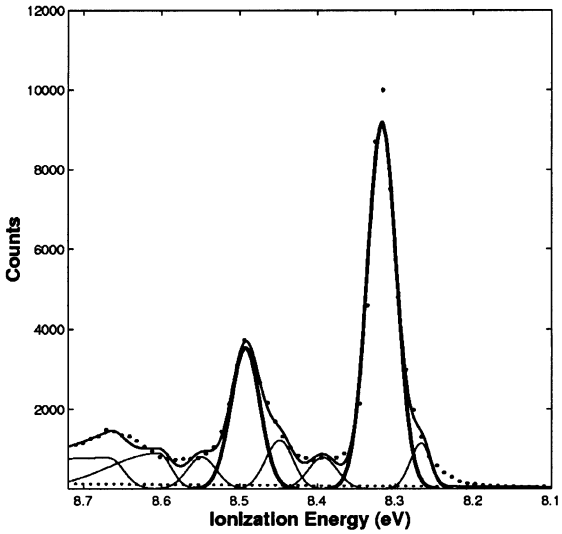

Figure 5. Low binding energy region in He I photoelectron spectrum of **3**. Experimental data (···) are fit with Gaussian functions corresponding to vibrational progressions (—) used in λ calculation on a baseline (···). Other Gaussian functions (−) describe spectral features of π_1.

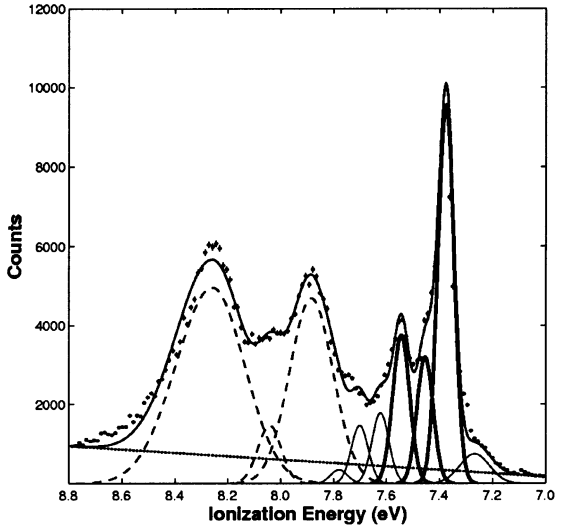

Figure 6. Low binding energy region in He I photoelectron spectrum of **4**. Experimental data (···) are fit with Gaussian functions corresponding to vibrational progressions (—) used in λ calculation, and π_2 and π_3 ionizations (- − -) on a baseline (···). Other Gaussian functions (−) describe spectral features of π_1.

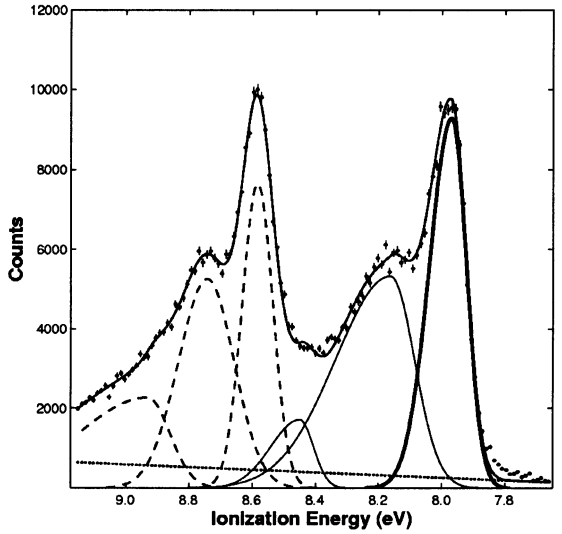

Figure 7. Low binding energy region in He I photoelectron spectrum of **5**. Experimental data (···) are fit with Gaussian functions corresponding to π_3 ionizations (- − -) on a baseline (···). Only one Gaussian function (—) is used in λ calculation. Other Gaussian functions (−) describe spectral features of π_1 and π_2.

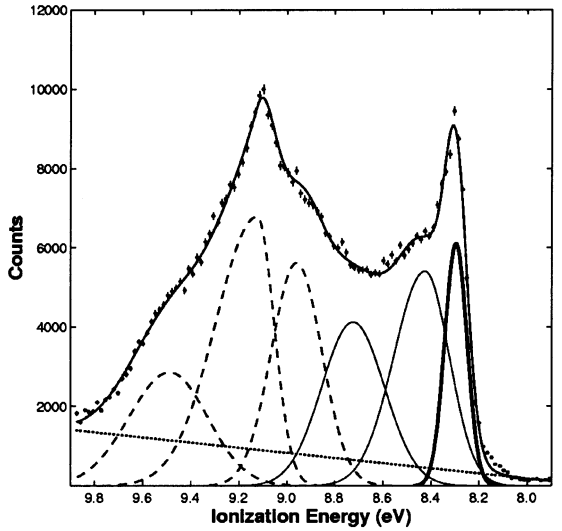

Figure 8. Low binding energy region in He I photoelectron spectrum of **6**. Experimental data (···) are fit with Gaussian functions corresponding to π_3 ionizations (- − -) on a baseline (···). Only one Gaussian function (—) is used in λ calculation. Other Gaussian functions (−) describe spectral features of π_1 and π_2.

and cation states (Table 2) can contribute to the breadth of individual vibronic lines in photoelectron spectra. Such band profiles are treated semiclassically (eq 4, IE is the ionization

$$G = |D|^2 e^{-(h\nu - \mathrm{IE})^2/4k_B T\lambda^{SC}} \quad (4)$$

energy and D is related to the transition moment).[24] The Gaussian functions, $T(\nu)$ (eq 1), that were used to fit the experimental spectra are convolutions of G (eq 4) and another Gaussian function, R, defined by the resolution of the instrument (eq 5).[25]

$$T(\nu) = \int_0^{\nu} G(x)\, R(x - \nu)\, dx \quad (5)$$

The value of H (the average full-width at half-maximum) for G was obtained by iterative reconvolution of the observed line-shape function and is related to λ^{SC}, according to eq 6. The results are summarized in Table 4.

$$\lambda^{SC} = \frac{H^2}{16 \ln(2)\, k_B T} \quad (6)$$

Reorganization Energies. Calculations employed B3LYP/6-31G(d,p) optimized geometries. B3LYP/6-311G++(2d,2p) single-point energies were calculated for four cases: (1) neutral optimized geometry, charge zero, and singlet multiplicity; (2) neutral geometry, charge plus one, and doublet multiplicity; (3) radical cation geometry, charge zero, and singlet multiplicity; and (4) radical cation geometry, charge plus one, and doublet multiplicity (Figure 9). The energy difference between (1) and (3) is λ^0, and the energy difference between (4) and (2) is $\lambda^{\bullet+}$. The latter parameter is compared to experimentally derived

TABLE 3: Vibrational Frequencies (cm^{-1}) and Quantum-Mechanical Reorganization Energies (meV)

	mode	ν(obsd)[a]	ν(calcd)[b]	ν(obsd)[c]	S[d]	λ^{QM}
1	$22a_1$	379 ± 34	405	408/398	0.692 ± 0.020	33 ± 3
	$10a_1$	1455 ± 34	1426	1431	0.636 ± 0.020	115 ± 4
2	$20a_1$	420 ± 34	408	408	$0.75\ 3 \pm 0.016$	39 ± 3
	$8a_1$	1461 ± 34	1450	1444	0.706 ± 0.015	128 ± 4
3	$5a_g$	1415 ± 34	1406	1403	0.387 ± 0.008	68 ± 2
4	$31a_1$	632 ± 34	632		0.334 ± 0.014	26 ± 2
	$16a_1$	1357 ± 34	1372	1360	0.393 ± 0.015	66 ± 3

[a] This work. [b] Calculated using B3LYP/6-31G(d,p). [c] See Table 2. [d] The values of S were obtained according to the expression: $S = (I_1 \pm \Delta I_1)/(I_0 \pm \Delta I_0)$, where ΔI_n is the square root of I_n.

TABLE 4: Experimental and Calculated Reorganization Energies (meV)

molecule	λ^{QM}	λ^{SC}	λ	$\lambda^{\bullet+}$	λ^0	λ^{total}	$2\lambda^a$
1	149 ± 5	21 ± 1	170 ± 5	107	105	212	340 ± 5
2	167 ± 5	13 ± 1	180 ± 5	129	143	272	360 ± 5
3	68 ± 2	22 ± 1	90 ± 2	54	77	131	180 ± 2
4	92 ± 4	66 ± 1	154 ± 4	57	65	122	316 ± 4
5	$(\leq 100)^b$	27 ± 9	$(\leq 127 \pm 9)^b$	71	76	147	$(\leq 254 \pm 9)^b$
6	$(\leq 100)^b$	16 ± 1	$(\leq 116 \pm 1)^b$	61	60	121	$(\leq 232 \pm 1)^b$

[a] Twice the observed reorganization energy for the self-exchange reaction. [b] Tentative assignment.

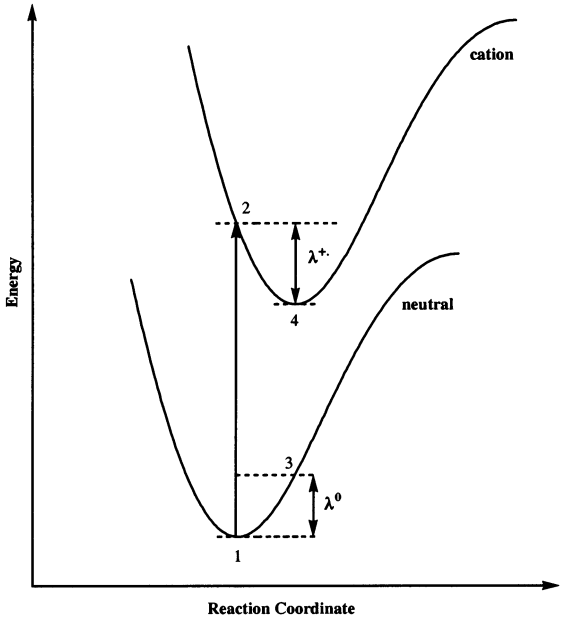

Figure 9. Potential energy surfaces of neutral and cation states that define $\lambda^{\bullet+}$ and λ^0.

values of λ in Table 4. The total reorganization energy, λ^{total}, for the $A + A^{\bullet+} \rightleftarrows A^{\bullet+} + A$ process is the sum of $\lambda^{\bullet+}$ and λ^0 (Table 4).

Discussion

Excellent agreement was obtained between experimental and calculated ionization energies for molecules **1** through **6** (Table 1). Koopmans' theorem gives raw calculated values for the first ionization energies that are roughly 0.1 eV lower than the experimental results. Shifting ionization energies such that the first experimental and calculated ionization energies are the same and then compressing the results by the factor of 1.3 produces excellent agreement (within 0.068−0.010 eV) with the experimental values.

Quantum-mechanical analyses of the first ionization bands of compounds **1**−**4** gave λ^{QM} values (Tables 3 and 4). The values for the vibrational spacings in the photoelectron spectra accord with calculated and experimental frequencies for the neutral molecules (Table 2). The frequency of the $22a_1$ mode in the spectrum of **1** is in excellent agreement with gas-phase IR data[20] and DFT calculations. The high-frequency vibrational spacing corresponding to the $10a_1$ mode also accords with experimental results and calculations.

Since the only difference between **1** and **2** is the presence of nitrogen atoms in ring positions 1 and 10, it is reasonable to expect that similar vibrational modes will be observed in the spectra of these molecules. Indeed, the $20a_1$ mode in the spectrum of **2** corresponds to the $22a_1$ mode of **1**. Moreover, the observed frequency is in good agreement with experimental and computational results. The high-frequency progression in **2** is spaced by 1461 ± 34 cm^{-1}, which is in excellent agreement with the $8a_1$ experimental and calculated vibrational frequencies (Table 2). The vibrational frequency of the $9a_1$ mode of **2**, however, corresponds to the observed $10a_1$ mode in the spectrum of **1**. The experimental frequency[21] of $9a_1$ in **2** is 1404 cm^{-1} (the calculated value is 1387 cm^{-1}). Given the relative error in the spacing of the high-frequency progression in the spectrum of **2**, the assignment to $9a_1$ is tentative. Unlike the $10a_1$ mode of **1**, however, there is only a 2 cm^{-1} difference between calculated $9a_1$ vibrational frequencies for the neutral and cation states of **2** (Table 2). For the $8a_1$ mode of **2,** the difference between neutral and cation states is 34 cm^{-1}. On the basis of these observations, we assign the observed high-frequency progression in the spectrum of **2** to $8a_1$, even though it does not correspond to the $10a_1$ mode of **1**.

A well-resolved vibrational progression in the spectrum of **3** corresponds to the $5a_g$ mode. Low-frequency progressions are also observed (Figure 5) and are used to fit the experimental data. These vibrational lines, however, are poorly resolved and were not used to estimate the reorganization energy.

The only five-ring molecule in the series that has a well-resolved high-frequency progression is **4**. We assign this progression (spaced by 1357 ± 34 cm^{-1}) to the $16a_1$ mode, and the low-frequency progression to $31a_1$. We estimate λ^{QM} to be 92 ± 4 meV, which is lower than λ^{QM} for **1** or **2**. We estimate λ^{SC} to be 66 ± 1 meV, which is larger than λ^{SC} for **1**, **2**, or **3**. If λ^{SC} is overestimated, it would explain the significant difference, 101 meV, between experimental and calculated reorganization energies.

Since the first and second ionization bands overlap in the photoelectron spectra of **5** and **6**, values of λ^{QM} were not obtained. Semiclassical band shape analyses give 27 ± 9 meV for **5** and 16 ± 1 meV for **6**. We assume that λ^{QM} is not greater than 100 meV. Therefore, we expect the total reorganization energy for **5** or **6** not to exceed 120−130 meV.

Calculated $\lambda^{\bullet+}$ values are lower than their experimental counterparts (Table 4). The best agreement is for **3**, where the difference between experimental and calculated parameters is only 36 meV. Computational results reproduce experimental trends in λ values (Table 4): λ and $\lambda^{\bullet+}$ for the three-ring

molecules are larger than those for the five-ring systems, with the exception of **3**. Ring systems containing heteroatoms exhibit larger λ and $\lambda^{\bullet+}$ values than their carbon analogues.

Calculated values of $\lambda^{\bullet+}$ and λ^0 are similar for **1**−**6** (Table 4), indicating that curvatures of the energy surfaces are equivalent for equilibrium geometries of neutral molecules and cations. We assume that curvatures of experimental parabolic surfaces for the neutral and cation species also are the same; therefore, total reorganization energies for the self-exchange electron-transfer reaction, $A + A^{\bullet+} \rightleftarrows A^{\bullet+} + A$, are 2λ (Table 4). With the assumption that solvent molecules do not perturb any of the internal modes involved in the self-exchange reaction, 2λ is the same as λ_i. The value of 2λ for **1** is 340 meV, and λ_i for intramolecular electron transfer between phenanthrene and the biphenyl anion radical is 450 meV.[3] Assuming that the reorganization energy of biphenyl is not greater than that of phenanthrene, λ_i for this reaction is only slightly higher than predicted from our results.

To extend the analysis to a single-ring system, we examined the reported He I photoelectron spectrum of benzene.[26] Unlike **1**−**6**, benzene has degenerate HOMOs and the first ionization energy is due to the removal of an electron from the $1e_{1g}$ π orbital.[27] Owing to the Jahn−Teller effect,[28] vibrational structure in the benzene spectrum is complex: the first band exhibits a strong adiabatic transition followed by short and weak progressions,[26] indicative of a small geometry change upon ionization. Treating the spectrum as for **1**−**6**, we estimate that λ does not exceed 100 meV. Calculations of the reorganization energy of benzene anion formation indicate that $\lambda^{\bullet-}$ is in the range 289−158 meV,[29] and reported changes in the bond lengths for the negative ion are almost the same as for the positive ion,[29] a finding supporting the assumption that $\lambda^{\bullet+} \approx \lambda^{\bullet-}$. The value of $\lambda^{\bullet-}$ for anthracene is in the range 67−86 meV,[29] which agrees well with our DFT calculation of $\lambda^{\bullet+}$, 57 meV, and experimental λ, 90 meV, of **3**. Since $\lambda^{\bullet-}$ for anthracene is nearly the same as $\lambda^{\bullet+}$ and λ of **3**, and $\lambda^{\bullet-}$ for benzene is slightly larger than 100 meV, our estimate of λ for benzene is reasonable. What is more, it is consistent with resonance Raman experiments of Myers and co-workers on the hexamethylbenzene/tetracyanoethylene complex, where the reorganization energy of specific modes localized on hexamethylbenzene is estimated to be 129 meV.[30]

Concluding Remarks

We have shown that mode-specific quantum-mechanical and semiclassical analyses of ionization band profiles can be used to determine electron-transfer reorganization energies for isolated molecules. Experimentally derived λ values for **1**−**6** are in the range 90−180 meV and are on average 63 meV higher than the DFT results. Reorganization energies of five-ring systems are slightly lower that those for three-ring systems. Analysis of the photoelectron spectrum of benzene yields $\lambda \leq 100$ meV.

Acknowledgment. This work was supported by NSF (CHE-0078809: H.B.G., J.R.W.; CHE-0078457: D.L.L.) and DOE (DE-FG03-95ER14574: D.L.L.).

References and Notes

(1) Balzani, V., Ed. *Electron Transfer in Chemistry*; Wiley-VCH Verlag GmbH: D-69469 Weinheim, Germany, 2001; Vols. 1−5.

(2) Marcus, R. A.; Sutin, N. *Biochim. Biophys. Acta* **1985**, *811*, 265−322.

(3) Miller, J. R.; Closs, G. L. *Science* **1988**, *240*, 440−447.

(4) (a) Chattoraj, M.; Laursen, S. L.; Paulson, B.; Chung, D. D.; Closs, G. L.; Levy, D. H. *J. Phys. Chem.* **1992**, *96*, 8778−8784. (b) Jortner, J.; Bixon, M.; Wegewijs, B.; Verhoeven, J. W.; Rettschnick, R. P. H. *Chem. Phys. Lett.* **1993**, *205*, 451−455. (c) Shou, H.; Alfano, J. C.; van Dantzig, N. A.; Levy, D. H.; Yang, N. C. *J. Chem. Phys.* **1991**, *95*, 711−713. (d) Brenner, V.; Millie, P.; Piuzzi, F.; Tramer, A. *J. Chem. Soc., Faraday Trans.* **1997**, *93*, 3277−3287. (e) Tramer, A.; Brenner, V.; Millie, P.; Piuzzi, F. *J. Phys. Chem. A* **1998**, *102*, 2798−2807. (f) Van Dantzig, N. A.; Shou, H.; Alfano, J. C.; Yang, N. C.; Levy, D. H. *J. Chem. Phys.* **1994**, *100*, 7068−7078.

(5) Balzani, V., Ed. *Electron Transfer in Chemistry*; Wiley-VCH Verlag GmbH: D-69469 Weinheim, Germany, 2001; Vol. 3, Part 2, p 177.

(6) Lichtenberger, D. L.; Kellogg, G. E.; Kristofzski, J. G.; Page, D.; Turner, S.; Klinger, G. Lorenzen, J. *Rev. Sci. Instrum.* **1986**, *57*, 2366.

(7) Renshaw, S. K. Ph.D. Dissertation, University of Arizona, 1992.

(8) Turner, D. W.; Baker, C.; Baker, A. D.; Brundle, C. R. *Molecular Photoelectron Spectroscopy*; Wiley-Interscience: London, 1970.

(9) *Jaguar version 4.0*; Schrödinger Inc.: Portland, OR, 1999.

(10) Frisch, M. J.; Trucks, G. W.; Schlegel, H. B.; Scuseria, G. E.; Robb, M. A.; Cheeseman, J. R.; Zakrzewski, V. G.; Montgomery, J. A., Jr.; Stratmann, R. E.; Burant, J. C.; Dapprich, S.; Millam, J. M.; Daniels, A. D.; Kudin, K. N.; Strain, M. C.; Farkas, O.; Tomasi, J.; Barone, V.; Cossi, M.; Cammi, R.; Mennucci, B.; Pomelli, C.; Adamo, C.; Clifford, S.; Ochterski, J.; Petersson, G. A.; Ayala, P. Y.; Cui, Q.; Morokuma, K.; Malick, D. K.; Rabuck, A. D.; Raghavachari, K.; Foresman, J. B.; Cioslowski, J.; Ortiz, J. V.; Baboul, A. G.; Stefanov, B. B.; Liu, G.; Liashenko, A.; Piskorz, P.; Komaromi, I.; Gomperts, R.; Martin, R. L.; Fox, D. J.; Keith, T.; Al-Laham, M. A.; Peng, C. Y.; Nanayakkara, A.; Challacombe, M.; Gill, P. M. W.; Johnson, B.; Chen, W.; Wong, M. W.; Andres, J. L.; Gonzalez, C.; Head-Gordon, M.; Replogle, E. S.; and Pople, J. A. *GAUSSIAN 98*, Revision A.9; Gaussian, Inc.: Pittsburgh, PA, 1998.

(11) Becke, A. D. *J. Chem. Phys.* **1993**, *98*, 5648−5652.

(12) Lee, C.; Yang, W.; Parr, R. G. *Phys. Rev. B* **1988**, *37*, 785−789.

(13) There is a simple procedure for scaling the raw calculated values (Martin, J. M. L.; El-Yazal, J.; Francois, J.-P. *J. Phys. Chem.* **1996**, *100*, 15358−15367) that accounts for anharmonicities provided that no strong Fermi resonances exist. We use ratios of computed to experimental frequencies of anthracene and phenanthrene as the desired scaling factors and report that they cluster in three groups: an average ratio of 0.956 for the C−H stretches; an estimated ratio of 0.973 for the in-plane bends; and an average ratio of 0.987 for the low-frequency in-plane vibrations. These scaling factors are then applied to the raw calculated frequencies of other molecules.

(14) Lichtenberger, D. L.; Copenhaver, A. S. *J. Electron Spectrosc. Relat. Phenom.* **1990**, *50*, 335−352.

(15) Koopmans, T. *Physica* **1933**, *1*, 104.

(16) Cornil, J.; Vanderdonckt, S.; Lazzaroni, R.; dos Santos, D. A.; Thys, G.; Geise, H. J.; Yu, L.-M.; Szablewski, M.; Bloor, D.; Lögdlund, M.; Salaneck, W. R.; Gruhn, N. E.; Lichtenberger, D. L.; Lee, P. A.; Armstrong, N. R.; and Brédas, J. L. *Chem. Mater.* **1999**, *11*, 2436−2443.

(17) Hush, N. S.; Cheung, A. S.; Hilton, P. R. *J. Electron Spectrosc. Relat. Phenom.* **1975**, *7*, 385−400.

(18) Brunschwig, B. S.; Sutin, N. *Comments Inorg. Chem.* **1987**, *6*, 209−235.

(19) Bree, A.; Solven, F. G.; Vilkos, V. V. B. *J. Mol. Spectrosc.* **1972**, *44*, 298−319.

(20) Cane, E.; Miani, A.; Palmieri, P.; Tarroni, R.; Trombetti, A. *Spectrochim. Acta A* **1997**, *53*, 1839−1851.

(21) Perkampus, H.-H.; Rother, W. *Spectrochim. Acta A* **1974**, *30*, 597−610.

(22) Durnick, T. J.; Wait, S. C., Jr. *J. Mol. Spectrosc.* **1972**, *42*, 211−226.

(23) Orr, S. F. D.; Thompson, H. W. *J. Chem. Soc.* **1950**, 218−221.

(24) Ballhausen, C. J. *Molecular Electronic Structures of Transition Metal Complexes*; McGraw-Hill: U.K., 1979; p 125.

(25) Press, W. H.; Flannery, B. P.; Teukolsky, S. A.; Vetterling, W. T. *Numerical Recipes, The Art of Scientific Computing, (Fortran Version)*; Cambridge University Press: New York, 1989; p 383.

(26) Karlsson, L.; Mattson, L.; Jadrny, R.; Bergmark, T.; Siegbahn, K. *Phys. Scr.* **1976**, *14*, 230−241.

(27) Hollas, J. M. *Modern Spectroscopy*, 3rd ed.; John Wiley & Sons Ltd: Chichester, U.K., 1996; p 270.

(28) Jahn, H. A.; Teller, E. *Proc. R. Soc. A* **1937**, *161*, 220−235.

(29) Klimkāns, A.; Larsson, S. *Chem. Phys.* **1994**, *189*, 25−31.

(30) Markel, F.; Ferris, N. S.; Gould, I. R.; Myers, A. B. *J. Am. Chem. Soc.* **1992**, *114*, 6208−6219.